

Proc. 4<sup>th</sup> Int'l Symp. on "The Air-Sea  
Interface", Sydney, Jan 1999.

## Wavenumber Spectra of Wind Waves in the Range of 1-50m

M.A. Donelan<sup>a</sup>, W.M. Drennan<sup>a</sup> & E. A. Terray<sup>b</sup>

<sup>a</sup> Rosenstiel School of Marine and Atmospheric Science,  
University of Miami, Division of Applied Marine Physics,  
4600 Rickenbacker Causeway, Miami, FL 33149-1098 USA  
e-mail: mdonelan@rsmas.miami.edu, wdrennan@rsmas.miami.edu

<sup>b</sup> Woods Hole Oceanographic Institution, Department of Applied  
Ocean Physics & Engineering, Woods Hole, MA 02543-1053 USA  
e-mail: eterray@whoi.edu

### Abstract

A new method of analysing wave directional data is applied to wave staff data from Lake Ontario during 106 episodes covering a range of wind speeds (up to 16 m/s) and significant heights (up to 2.5m). The method yields wavenumber spectra directly and examples are shown of downwind slices through the full 2-D wavenumber spectrum. These spectra are steeper than the conventional view would suggest, tending asymptotically to  $k^5$  at high wavenumbers with respect to the peak. On the other hand, the spectral peaks of the individual runs follow a steepness limited  $k^{-4}$  pattern.

### 1 Introduction

The resolution of many issues regarding the mechanics of the air-sea interface lies in knowledge of the details of the wavenumber spectrum of surface waves. Such issues include: the calculation of the interfacial friction coefficient; the modelling of wave propagation; remote sensing of winds, waves and surface topography; acoustic absorption and scattering in the upper ocean layers; kinetic energy dissipation and upper layer mixing. In spite of the fundamental importance of the wavenumber spectrum direct measurements of it have so far been in short supply. Airborne scanning optical or radar ranging devices are beginning to accumulate data sets, but no consistent description of the wavenumber spectrum of wind generated seas has yet emerged.

**DISTRIBUTION STATEMENT A**  
Approved for Public Release  
Distribution Unlimited

DTIC QUALITY INSPECTED 4

19990709 056

In this paper we employ a new method of *in situ* measurement of wave directional properties to determine the general behaviour of the wavenumber spectrum in the range of 1m to 50m. The method, which is described in Donelan *et al.* (1996), uses wavelet analysis of time series from wave staffs at 3 or more points arranged so that the included angle is in the vicinity of 90 degrees. The phase differences between pairs of staffs are combined to yield instantaneous vector wavenumber and associated amplitude in each frequency bin. The method, called the Wavelet Directional Method (WDM), yields very high resolution directional information that is insensitive to the accuracy of the calibration of the individual wave staffs.

A complex wavelet transform applied to the time series obtained from each wavestaff yields a set of wavelet coefficients that are functions of both time and apparent scale (the latter corresponding roughly to the encounter frequency). The physical stratification of the "spectral content" of the data in time affords the advantage of considerably reducing the complexity of the directional estimation problem, since it is most probable that only a single group is present at the measurement array at any one time. We justify this assumption by the a posteriori observation that the directional spread obtained by this method is only slightly smaller than that obtained by other means (Donelan *et al.*, 1985). The penalty paid for the temporal resolution is a corresponding decrease in scale resolution. However, since the component wavelets are themselves compact, they still provide a parsimonious representation of the "groupiness" seen in the measurements.

Under the assumption that only a single wave group is present at any time,  $t$ , the phase between the  $i^{th}$  and  $j^{th}$  staffs is given by

$$\phi(t)_{ij} = k_x(t)X_{ij} + k_y(t)Y_{ij}$$

where  $(X_{ij}, Y_{ij})$  denotes the relative X-Y separation of the pair. This system of equations can be solved for the magnitude and direction of the wavenumber  $\mathbf{k} = (k_x, k_y)$ . Since, in principle, a solution can be obtained using just two pairs of staffs that are not co-linear, multiple estimates of  $\mathbf{k}$  are available (*i.e.* the system is overdetermined), and therefore it is also possible to determine the random error in the estimate of  $\mathbf{k}$ . The energy of the wave is given by the magnitude-squared of the corresponding wavelet coefficient, and the directional spectrum built up by weighting the energy by the number of arrivals in each wavenumber bin.

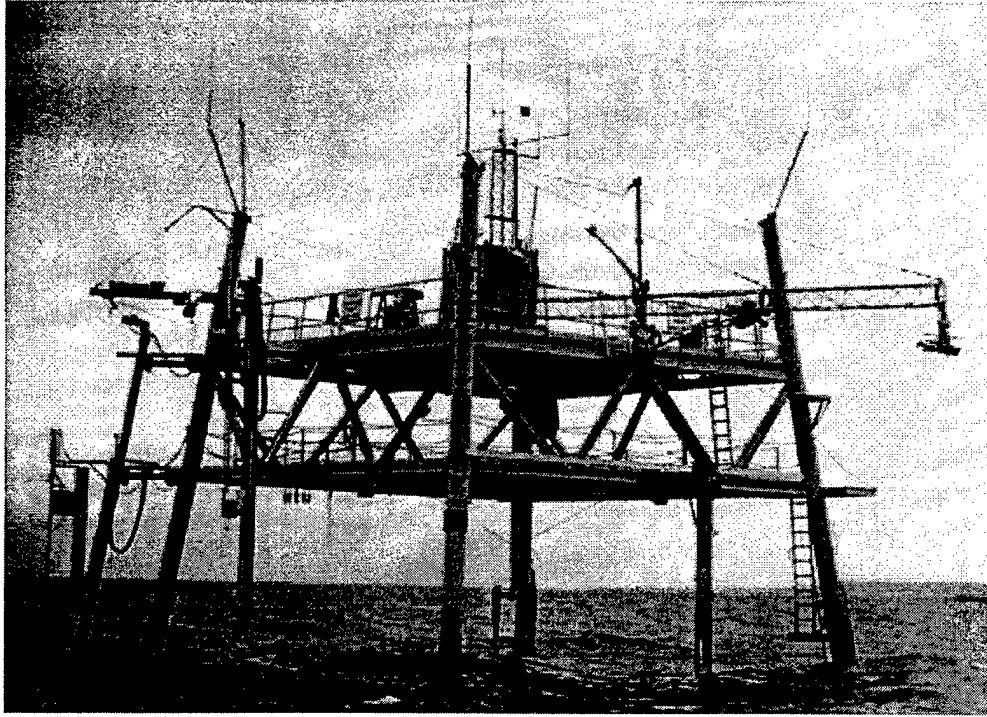


Figure 1: View from the north-west of the research tower of Canada's National Water Research Institute at the western end of Lake Ontario. The array of wave staffs is attached to the underside of the lower deck on the east face.

## 2 The Data

The data analysed by this method were obtained from the research tower of Canada's National Water Research Institute at the western end of Lake Ontario (Figure 1). The tower stands in 12m of water and is exposed to a range of fetches from 1.1 km in westerly winds to 300 km in easterly winds. Waves were measured by means of an array of 6 capacitance wave staffs arranged in a centered pentagon of radius 25cm. The wave staffs were 6m long and were sampled at 20 Hz with a resolution of 1.5 mm. The data were collected over the fall (October to December) of 1987 in runs of length 95 minutes. There were 106 runs covering the full range of fetches (1.1 to 300 km), wind speeds of 1 to 16 m/s and significant heights of 0.1m to 2.5m.

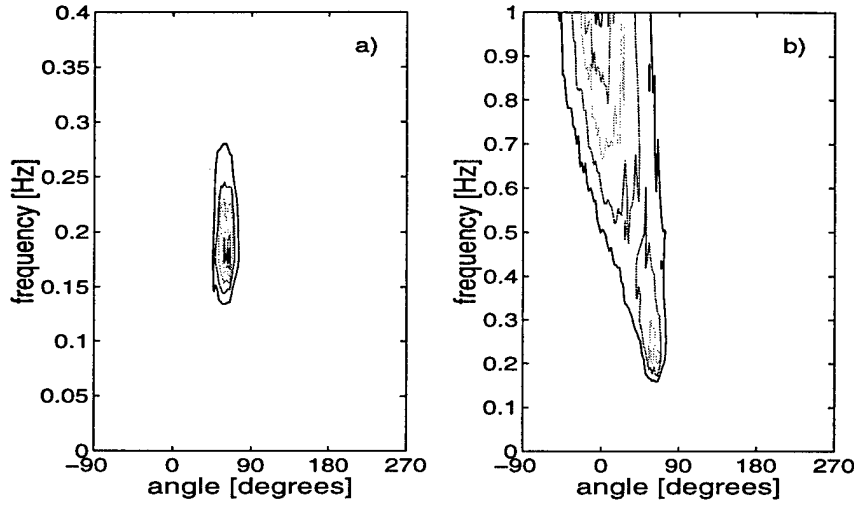


Figure 2: Panel a) frequency-direction spectra,  $F(f, \theta)$ , for a well-developed wave field. Panel b) as in panel a) but with spectral estimates pre-whitened by multiplying by  $f^5$ .

### 3 Results

#### 3.1 Directional spreading

Fig. 2 shows a typical frequency direction spectrum for winds from the north. The waves have a peak period of 6.5 seconds. The WDM produces compact well-defined spectra, in which (panel b) spreading at high frequencies, with respect to the peak, is evident. Note that, while the short waves (0.8 to 1.0 Hz) are spread uniformly about the wind direction ( $-4^\circ$ ), longer waves tend to come from the direction of longest fetch (*c.f.* Donelan *et al.* 1985). The spreading function deduced from earlier data analysed with a different approach (Donelan *et al.* 1985) is applied to these data in the wavenumber-direction space:

$$D(k, \theta) = \frac{\beta}{2} \sec^2 \beta (\theta - \theta_{\max}(k)) \quad (1)$$

Fig. 3 shows  $\beta(k)$  for a case of strong winds from the west;  $U = 11$  m/s; the ratio of wind speed to phase speed of the waves at the spectral peak,  $U/c_p = 4.1$ . As noted before (e.g., Donelan *et al.* 1985) the narrowest spreading (largest  $\beta$  values) is near the peak and the spreading rapidly increases at higher and lower frequencies. Since the ratio of the integral over

all directions ( $\pm\pi$ ) to the downwind value ( $\theta = \theta_{\max}$ ) is proportional to  $\beta^{-1}$ , this is plotted in Figure 3b. The linear increase in spreading with  $k/k_p$  is evident from  $1 < k/k_p < 5$ .

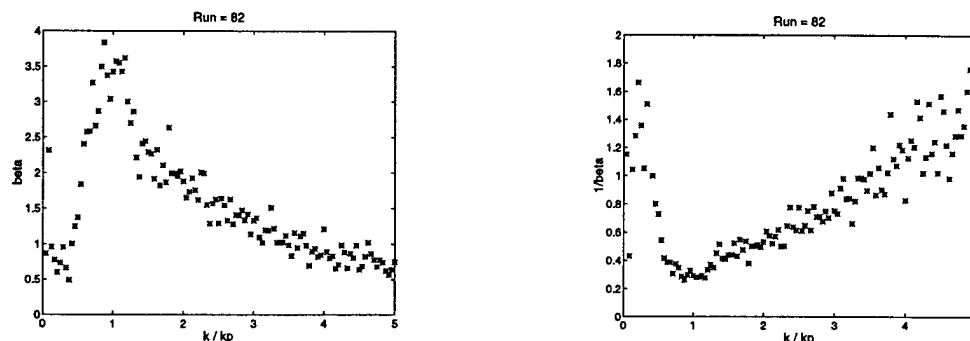


Figure 3: Left panel: the argument,  $\beta$ , of the  $\text{sech}^2$  spreading function in the wavenumber spectrum for a case of strongly forced waves at short fetch. Right panel: the inverse of  $\beta$ . Both plots are versus relative wavenumber,  $k/k_p$ .

### 3.2 Doppler shifting

Of course, the conversion of wavenumber spectra to frequency-of-encounter spectra must allow for the effects of Doppler shifting of the short waves by the orbital velocities of longer waves. This is clearly seen in Figure 4 which shows the frequency of occurrence of various wavenumbers for selected apparent frequencies under the combined time-dependent advection of currents and longer wave components. The longer wavenumbers in a given frequency band are Doppler shifted up on the crests of even longer waves, while shorter waves are Doppler shifted down in frequency in the reverse flow of the troughs.

The overall effect is the spreading of observed wavenumbers well outside the limits of the dispersion relation corresponding to edges of the frequency band. The Doppler shifting becomes more pronounced as one moves up the spectrum to higher frequencies and shorter waves. Note also that the mode of the distribution, corresponding to the most frequently occurring orbital speed plus drift speed, is shifted to the left of its expected value from the linear dispersion relation. Since the Eulerian orbital velocities are closely Gaussian their mode is at zero and therefore the shift of the mode in Figure 4 must correspond to the wind drift velocity and Stokes drift together. Thus the wave field, analysed in this way, provides an excellent indication of the

current profile with depth, the longer waves feeling the currents at greater depths (Stewart and Joy, 1974). This approach will be explored further in subsequent work.

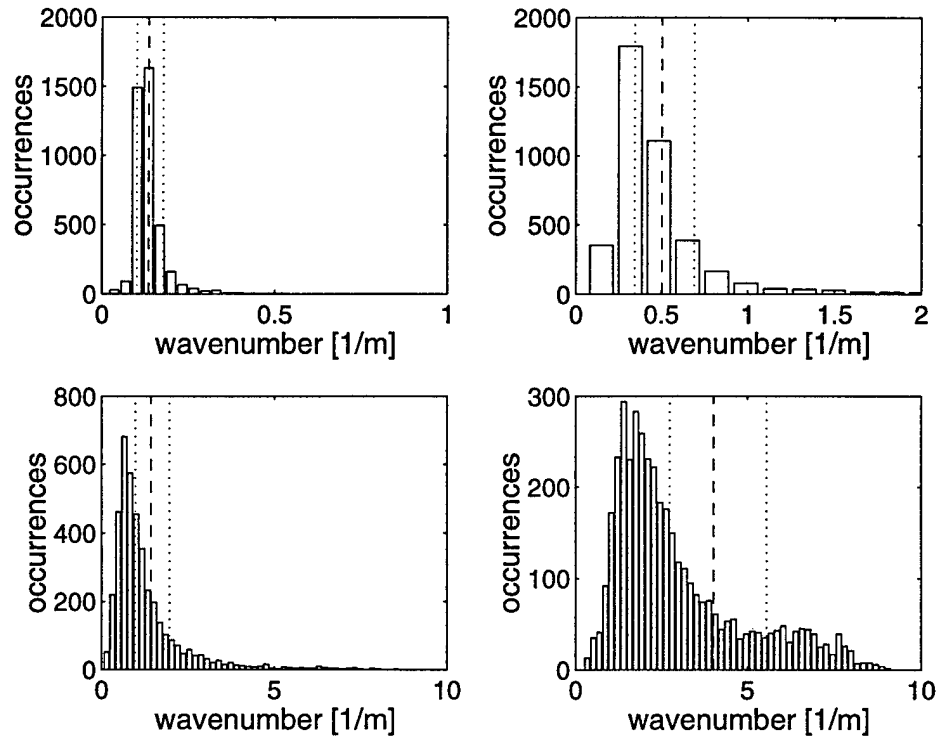


Figure 4: Histograms of the observed wavenumbers in particular frequency bands. The dashed line is at the location of the wavenumber corresponding to the linear dispersion relation at the center frequency of the band. The dotted lines are the locations corresponding to the edges of the band. The center frequencies are 0.177, 0.354, 0.595 and 1.000.

### 3.3 2-D wavenumber spectra

Two examples of downwind slices through the 2-D spectrum are shown in Figure 5. The panels illustrate spectra in strong wind conditions but very different fetches. In both cases the dashed line corresponds to a slope of  $k^{-5}$  with no change in the multiplier. It is apparent that the longer fetch (better developed) spectra (5b) are lower in the high wavenumber range (1 rad/m to 6 rad/m) and they fall off less rapidly. That is, there is no traditional equilibrium range in the 2-D wavenumber spectra.

Cox and Munk (1954) have derived mean square slopes of wind-generated waves from sun glitter. These results are generally considered to be the benchmark against which slopes computed from wavenumber spectra are to be evaluated. The mean square slopes of Cox and Munk for oil-slicked surfaces corresponds (by their calculation) to the slopes of waves of length 39 cm ( $k = 16$  rad/m) and longer. Our spectra are evaluated to  $k = 6$  rad/m. If they are extended, with the slope of the wavenumber range 2 to 6 rad/m, to  $k = 16$  rad/m the calculated mean square slopes are in reasonable agreement with those of the slicked surfaces observed by Cox and Munk.

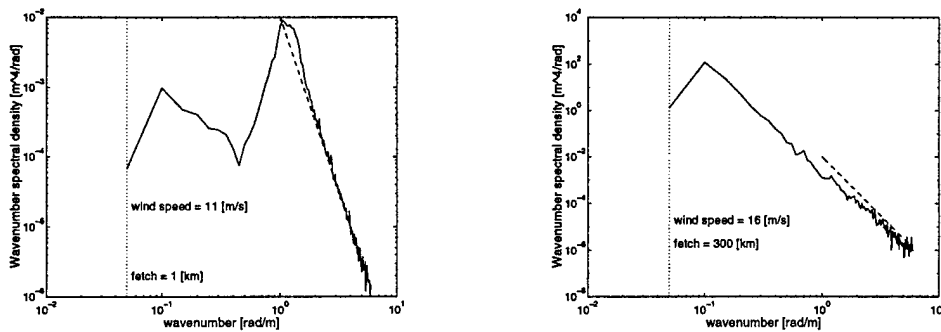


Figure 5: 10 degree slices, centered on downwind, of the full 2-D wavenumber spectrum for strong winds. Left panel: short fetch, strong forcing. Right panel: long fetch, well-developed waves. The dashed lines shown are  $0.01 k^{-5}$ . The vertical dotted line is drawn at the wavenumber with phase propagation speed equal to the wind speed.

### 3.4 Spectral peaks

Are the waves at the spectral peak limited by steepness in the manner described by Phillips (1958) for the "equilibrium range"? In Figure 6 the peak of the 2-D wavenumber spectrum in the downwind direction is plotted versus wavenumber for those cases where the wind speed was above 4 m/s. The solid line has a slope of  $k^{-4}$  and the regression line (dashed) of  $k^{-3.8}$ .

## 4 Conclusions

We have applied a new method of analysis to surface waves and obtained direct estimates of wavenumber spectra and spreading functions about the peak propagation direction. The results show that the spreading increases uniformly away from the peak in both directions, and the 2-D wavenumber spectra do not exhibit an "equilibrium range" in which the spectral shape is invariant. On the other hand, the spectral density of the peak of individual

cases lies along a  $k^{-4}$  line suggesting that waves at the peak of the spectrum propagating downwind are limited by steepness, while the shorter waves in the system are affected by other processes such as hydrodynamic straining and wave-wave interactions. We are conducting further analyses along these lines to determine if these results apply to a wider range of conditions.

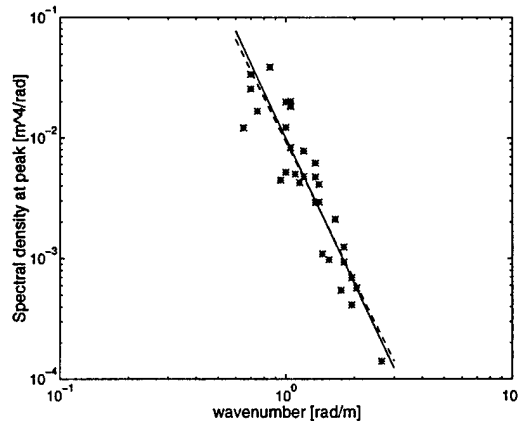


Figure 6: Spectral density at the peak of wavenumber spectra in the downwind direction for individual cases with varying peak wavenumber. The dashed line is the regression line of slope  $k^{-3.8}$  and the solid line has slope  $k^{-4}$ .

## Acknowledgements

We gratefully acknowledge the contribution of many members of the engineering and technical staff of NWRI in the design, construction and operation of the apparatus. MD and WD acknowledge ONR support through grant N00014-97-1-0015. ET acknowledges support from NSF grants 9521002, 9713160 and ONR grants N00014-98-1-0793, N00014-97-1-0483.

## References

1. Cox, C., and W. Munk, 1954: Statistics of the sea surface derived from sun glitter. *J. Mar. Res.*, **13**, 198-227.
2. Donelan, M.A., W.M. Drennan and A.K. Magnusson, 1996: Non-stationary analysis of the directional properties of propagating waves. *J. Phys. Oceanogr.*, **26**, 1401-1414.
3. Donelan, M.A., J. Hamilton and W.H. Hui, 1985: Directional spectra of wind generated waves. *Phil. Trans. R. Soc. London*, **A315**, 509-562.
4. Phillips, O.M., 1958: The equilibrium range in the spectrum of wind-generated waves. *J. Fluid Mech.*, **4**, 426-434.
5. Stewart, R.H., and J.W. Joy, 1974: HF radio measurements of surface currents. *Deep Sea Res.*, **21**, 1039-1049.